



Evaluation of Energy Recovery from Laboratory Experiments and Small-scale Field Tests of Underground Coal Gasification (UCG)*

by Faqiang SU¹, Ken-ichi ITAKURA^{2*}, Gota DEGUCHI³,
Koutarou OHGA⁴ and Mamoru KAIHO⁵

Cavity growth occurring with crack extension and coal consumption during UCG processes directly influences the gasification efficiency and the estimated subsidence and gas leakage to the surface. This report presents an evaluation of the gas energy recovery, coal consumption, and gasification cavity estimation using a proposed stoichiometric method to analyze the coal gasification reaction process. We defined the evaluation parameters of rate of energy recovery and investigated the effects of different parameters using UCG trials conducted with coal blocks and coal seams, adopting different Linking-hole methods and operational parameters.

Analyses of results obtained from laboratory experiments and small-scale field trials using V-shaped and L-shaped linking holes, and Coaxial-hole UCG models show that the gasification of Linking-hole models yielded average calorific values of product gas as high as 10.26, 11.11 MJ/m³ (lab.), and 14.39 MJ/m³ (field.). In contrast, the Coaxial-hole models under experimental conditions yielded average calorific values of product gas as: 7.38, 4.70 MJ/m³ (lab.) and 6.66 MJ/m³ (field.). The cavity volume obtained with Coaxial models was about half of the volume obtained from Linking-hole models. Results obtained for these UCG systems show that the feed gas and linking-hole types can influence coal consumption and product gas energy. Fissure ratios were also investigated. Results confirmed major factors underpinning gasification efficiency. Linking-hole types strongly influenced the development of the oxidization surface and fracture cracks for subsequent combustion in the gasification zone.

Estimated gas energy recovery results support experimental observations within an acceptable error range of about 10%. Moreover, this stoichiometric approach is simple and useful for evaluating the underground cavity during UCG. Based on these results, we proposed a definition of the energy recovery rate, combined with the obtained volumes of gasification cavities that provide a definition of energy recovery and UCG effects.

KEY WORDS: Underground Coal Gasification, UCG Model, Gasification Effect, Coal Consumption, Energy Recovery

1. Introduction

Coal, the most abundant fossil fuel resource in the world, has proven reserves that are expected to be primary energy source for the 21st century. From the perspectives of safety and efficient resource utilization, coal is the subject of great expectations to satisfy the rapidly increasing demand for energy. As a clean coal technology, Underground Coal Gasification (UCG) is used to create a combustion reactor in an underground coal seam, thereby enabling the collection of heat energy and gases (hydrogen, methane, etc.) through the same chemical reactions that are used in surface gasifiers. As early as 1912, the

first plan for UCG experiments was proposed by Sir William Ramsay. They were conducted on a small-scale in Durham, UK¹⁾. A field study of UCG technology was done in the 1930s in the Union of Soviet Socialist Republics (USSR)¹⁾. The technology was developed to a limited degree in the US, Europe, China, and Japan later during the 1960s and 1970s²⁻¹⁰⁾. However, many countries have recently shown increased interest in this method: modern sensing and control techniques can reduce UCG environmental effects by curtailing greenhouse gas emissions to the air and by leaving no ash aboveground.

The relevant literature describes experimental tests and modeling experiences of UCG that have been pursued in recent decades. Theoretical and experimental studies have increased year-by-year in many countries since the 1930s^{1, 11-14)}. A typical UCG system is presented in Fig. 1. It includes a coal seam with two boreholes drilled down into it: one for injecting reaction gas for in-situ burning of coal and the other for extracting the product gas. Actually, UCG minimizes health hazards and improves miners' safety because it requires no underground work, eliminates environmental hazards, and

*Received 29 September, 2014; accepted for publication 10 April, 2015

1. Center of Environmental Science and Disaster Mitigation for Advanced Research, Muroran Institute of Technology

2. Graduate School of Engineering, Muroran Institute of Technology, 27-1 Mizumoto, Muroran, 050-8585, Japan

3. Underground Resources Innovation Networks, NPO

4. Graduate School of Engineering, Hokkaido University

5. National Institute of Advanced Industrial Science and Technology, Energy Technology Research Institute

[For Correspondence] E-mail: itakura@mmm.muroran-it.ac.jp

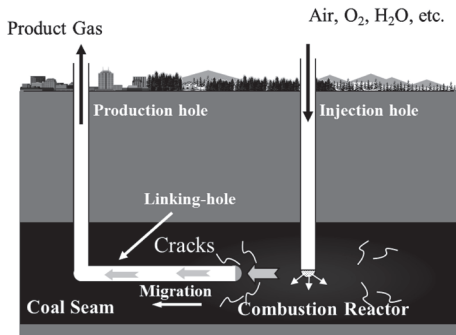


Fig.1 Schematic of underground coal gasification system.

offers important benefits for deep and thin coal seams that have not been economically feasible to mine. Nevertheless, several important shortcomings must be avoided: gas leakage, surface subsidence, and especially the potential pollution of underground water.

With UCG, an underground reactor is created. It expands around the linking hole, i.e. the gasification channel. This paper introduces the UCG trials with distinct Linking-hole models and the Coaxial-hole models, which can be suitable for different conditions of coal deposits and geological structures of the underground coal seams. Herein, we assess the influences of some linking methods, feed gases and gas flow rates on both the product gas composition and gasification efficiency. The research goals for the experimental studies are to ascertain those factors' potential benefits, elucidate the evolution of the gasification cavity, and assess the effects of various design and operational parameters.

The cavity volume left by coal that has burned underground and the amount of coal consumption are complex phenomena that cannot be readily observed in-situ. Moreover, it is difficult to simulate actual coal gasification precisely by application of reliable scientific analysis of fundamental experiments. The cavity volume and coal consumption have been regarded as important parameters for evaluating the gasification effect. The coal combustion produces the underground cavity, which grows continuously during the UCG process. The cavity development is governed by its extent and the reaction rate prevailing in the reactor. Data related specifically to the product gas energy of underground gasification reactors are scarce.

For the precise control and evaluation of the gasification zone, and for improving efficient and environmentally friendly UCG systems, this study provides a stoichiometric approach to evaluate the coal gasification reaction process and analyze product gases from the obtained product gas compositions. Using the designed UCG experiments, we ascertained the gasification rate and investigated the effects of linking-hole types and the effects of feed gas on gasification efficiency to characterize energy recovery and cavity growth. We also verified the effectiveness of the proposed stoichiometric approach.

2. Experimental

Experiments consisted of atmospheric gasification using

Table 1 Proximate analysis and ultimate analysis of coal.

No.	Parameter	Kushiro Coal	Sunago Coal
Proximate analysis (%)			
1	Fixed moisture	6.10	3.20
2	Ash content	14.50	17.42
3	Volatile matter	42.9	37.97
4	Fixed carbon	36.5	41.41
5	Total sulfur	0.17	2.05
Ultimate analysis (%)			
6	Carbon	65.53	81.85
7	Hydrogen	5.47	6.08
8	Nitrogen	1.03	1.98
9	Oxygen	12.49	9.99
10	Calorific capacity (MJ/kg)	26.15	25.43

V-shaped, L-shaped linking-hole models and Coaxial-hole models, under conditions of underground gasification. The ex-situ reactors used air, oxygen or their mixture as gasification agents.

2 · 1 Coal Samples Preparation and Experimental Design

Coal blocks used in the laboratory were shaped into rectangular prisms, which were supplied by the Kushiro Coal Mine (Japan) . Results of the proximate analysis and ultimate analysis (C, H, N, O compositions) of the coal samples and coal seam used in the field study are given in Table 1. The coal used for the in-situ study has high sulfur (2.05%) content. The ash contents were high: 14.50% and 17.42%. It might be readily apparent that the two types of coal have similar calorific value (nearly 26 MJ/kg) and low moisture (3–6%) .

Coal combustion experiments were conducted to evaluate gasification effect in the coal blocks using types of designated UCG Linking-hole models. The model design is viewed as the key step for a feasibility study. It provides a reliable reference for gasification processes on a field scale. Along with the development of the UCG technology, many design approaches have been developed for the underground reactor structure. After an underground reactor is created, it expands around the linking hole, forming a gasification channel. In a typical UCG system, two wells, designated for injection and production, are drilled from the surface into a coal seam at some distance apart. An underground gas channel connects the wells by various linking techniques¹⁵⁻¹⁷⁾. However, it is difficult to apply a universal UCG system directly to an underground coal seam having a complex geological structure.

An underground link between the two wells must be established within the coal seam because the underground primitive conditions, surrounding rock characteristics, and coal properties cannot readily provide a porous gasification channel for gas flow and continuation of the reaction¹⁸⁾. Consequently, for the specific burial conditions of each coal

Table 2 Outline of UCG laboratory experiments.

No	Molded material	Coal types	Configuration	Operation time, h	Gasification agents
P2	Concrete+ Drum (20L)	Kushiro	V-shaped	8.0	Oxygen
P6	Concrete+ Drum (20L)	Kushiro	Coaxial-hole	5.2	Oxygen
P7	Concrete+ Drum (20L)	Kushiro	L-shaped	8.4	Oxygen
P8	Concrete+ Drum (20L)	Kushiro	Coaxial-hole	8.7	Oxygen+ Air
F1	Outcrop coal 1 302×h 140 cm	Sunago	Linking-hole	38.8	Oxygen
F2	Outcrop coal 1 354×h 101 cm	Sunago	Coaxial-hole	9.0	Oxygen

deposit, the best corresponding linking methods should be used. This study designed and applied UCG works with three link methods, namely, V-shaped¹⁹⁾ and L-shaped linking-holes and Coaxial-hole UCG models were designed and conducted. The V-shaped model is similar in form to the “long-wall” controlled retractable injection point (CRIP) developed in the 1980s by Lawrence Livermore National Laboratory (LLNL)^{1, 17)}. In the L-shaped model, the production well is drilled from the surface to connect the borehole bottom of injection well. The ignition position can be set in a specific location. The two wells can also be designed to have different cross angles that depend upon the diverse distribution and disposition of coal seams. Coaxial UCG models are anticipated for use in small communities as a local energy source because the costs to construct the drill hole and ground plant facility are lower than those for conventional UCG with a linking hole.

Table 2 presents data related to the molded materials and main operating conditions of the typical laboratory experiments with a drum can and small-scale field tests conducted for our study. This study examined V-shaped and L-shaped linking-hole models, and Coaxial-hole models. The gasification process was controlled by adjusting the injection gas (air/O₂), based on the product gas concentration and temperature profile. For instance, the feed gas flow rate will be increased when the concentration of the combustible gas components (e.g., CO, CH₄) decreases or the reactor temperature declines. Two small-scale in-situ field tests were conducted with oxygen using Linking-hole and Coaxial-hole models.

The general structure of the gasifier applied in the laboratory simulations of underground gasification is presented in Fig. 2. The experimental setup is equipped with the gasification simulated UCG model (see Fig. 3), a gas agent supply system, and a gas chromatographic analyzer for analyzing the gas production compositions. The acoustic emission (AE) activities occurring around the UCG reactor were recorded using an AE waveform recorder. The AE reflect the crack generation during gasification. The results of AE activity analyses are explained in a later report. The load cell

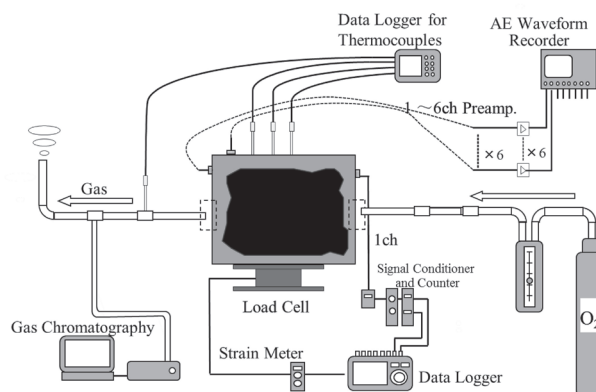


Fig.2 Scheme of the experimental setup.

was applied for measuring the weight loss of the UCG model with respect to the operation time. A drain tank was mounted at the gas production hole for filtering the tar and water. At a specified time interval, some dry and clean gaseous products were sampled to the gas chromatograph for chemical analyses.

2 · 2 Process Monitoring

The sections and dimensions of the UCG models reported in this paper are given in Fig. 3. In the ex-situ model, the underground conditions can be simulated both with respect to the coal seam and the surrounding rock layers. The reactor walls were made of heat-resistant concrete of a certain thickness. Coal samples were designed in a rectangular prism shape and were cast in the drum can ($\phi 27.5 \times 36$ cm) with the concrete. The positions of the thermocouples mounted inside the models are denoted as “channel (CH)” in the Figs. This Fig. shows V-shaped and L-shaped linking holes, and a compact coaxial pipe were set in the models for injecting the gasification agents and for extracting the product gases. The 22-mm-diameter injection hole of the L-shaped model was drilled for convenient ignition. It does not affect the gas flow rate. As portrayed in the Coaxial UCG model, a coaxial thin inner tube, which was used for injecting air/oxygen, was able to slide up and down to adjust the outlet position for advancing the gasification zone stepwise. The outer pipe (the annular space formed between the inner pipe

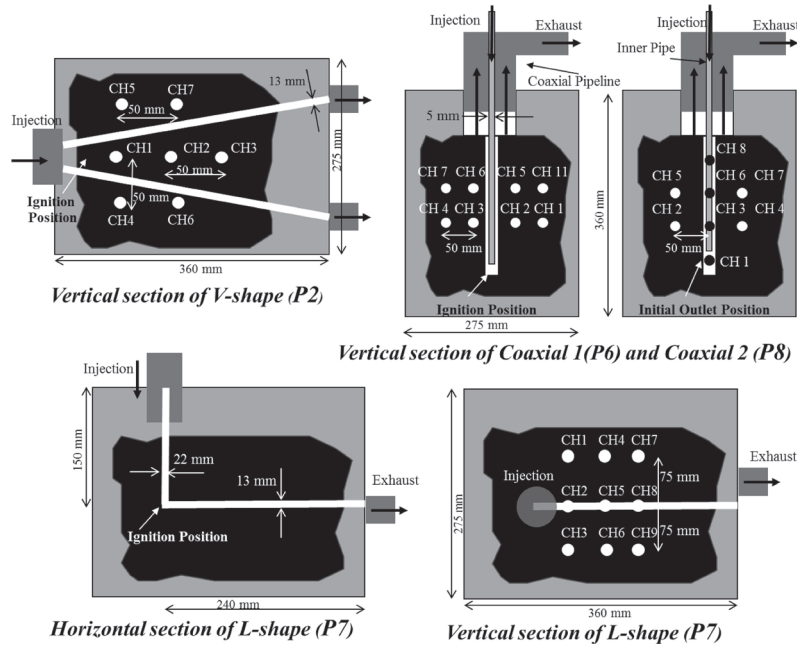


Fig.3 Dimensions and cross-sections of simulated UCG reactors.

and coaxial-pipe) serves as a gas production hole.

To control the temperature profiles in the gasified coal block, the model was equipped with a set number of thermocouples, which were deployed as presented in the Fig.. Such information is crucial for controlling the process development and cavity growth.

At the start of the experiment, the coal block was ignited with a gas burner and burning charcoal fragments in the ignition location, which produced a sufficiently high-temperature environment; then, the gas agent supply system was connected to the inlet position. The ignition process, which was managed in real time by temperature measurements, normally lasted about 10 min. During heating, the temperature on the thermocouples located near the ignition area increased rapidly and reached around 800–1000 °C ; at which time the coal ignition was considered complete. The temperature changes, production gas contents, and model weights were measured successively after igniting the coal and blowing air or oxygen at different flow rates.

The hot product gas was passed through the drain tank in which steam and other condensable gases were trapped. Dry and clean product gases were sampled and sent to the gas chromatograph for the quantitative analysis of components every 10 or 20 min. The sampling interval was changed as necessary (e.g. adjustment of processing parameters or the special time points) . The method of calculating the calorific value of the product gas stream is described in the Discussion section.

3. Results

3 · 1 Coal gasification with Designed UCG Models

3 · 1 · 1 V-shaped Linking-hole Model (P2) After the ignition process, the gasification agent supply system was equipped to the UCG reactor. Then, for the next 8 h, pure oxygen was supplied into the reaction zone at an average flow rate of about 5 L/min.

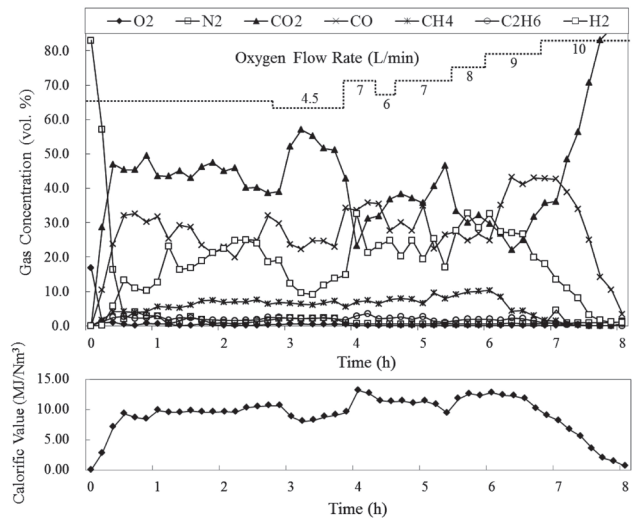


Fig.4 Changes in the product gas concentration during gasification (P2).

Fig. 4 presents the percentage compositions and calorific value of the gaseous products with respect to the operation time, as obtained from a single experiment with a V-shaped linking-hole model. Results obtained for the initial combustion period indicate that N₂ accounted for more than 80%. It dropped gradually along with the CO₂ composition increase. At about 25 min after beginning the experiment, the gas stream was ignited successfully. During the subsequent period of about 3 h, the combustion area underwent continuous stable gasification. The quality of gas obtained in the phase (3–4 h) was low. It mainly comprised CO₂, which was the main component (57.1%) ; the CO and H₂ contents showed a downward trend. The calculated calorific value of the product gas was 8.03 MJ/m³ at this time. Consequently, the oxygen supply rate was increased to 7 L/min; the CO, H₂ composition exhibited a marked increase thereafter. The calorific value also reached a peak value (13.19 MJ/m³) at

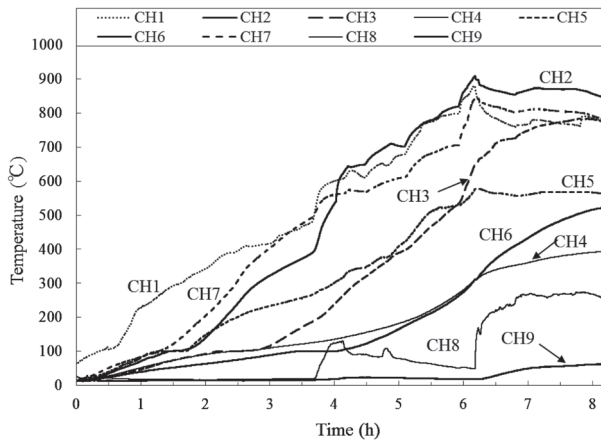


Fig.5 Temperature profile with operational time (P2).

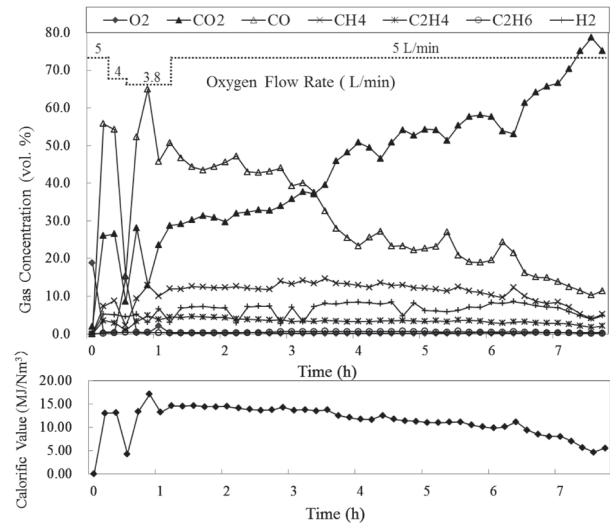


Fig.6 Changes in product gas concentrations during gasification (P7).

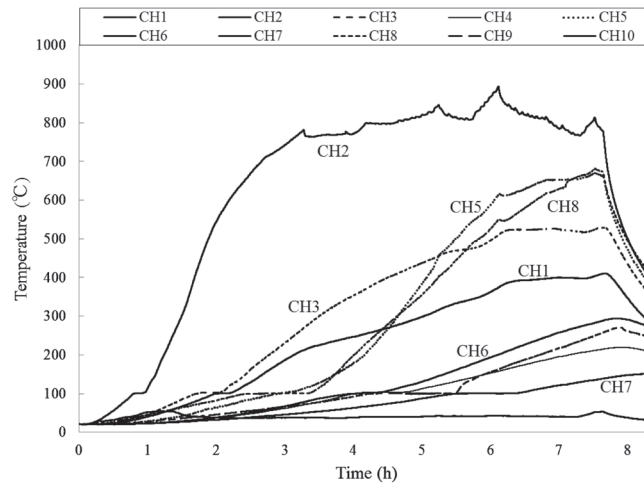


Fig.7 Temperature profile with the operational time (P7).

4 h. During the latter period of the experiment, the combustible gas compositions decreased and the ratio of CO₂ continued to rise in spite of the increase of the oxygen supply rate. In fact, CO, H₂, and CH₄ were produced continuously throughout the entire process. The average calorific value estimated from these gas compositions was about 10.26 MJ/m³.

Temperature changes taking place inside the model during the experiment are presented in Fig. 5. The rates of temperature increase of each thermocouple and the high-temperature areas are clearly visible in this Fig.. In the gas-exhaust passage, the CH8 and CH9 thermocouples were mounted for detecting the temperatures of the product gas stream. During the initial part of the experiment, the temperature around the ignition area (CH1) increased. The higher zone moved along the upper linking-hole (CH2, CH7) in the middle period. During the latter period, the temperature around the lower linking-hole (CH3, CH6) increased abruptly. After about 2.8 h, the temperature recorded at each thermocouple rose slowly. The percentage of combustible gas contents and their calorific value decreased. Corresponding to the same position of 4 h around in Fig.

4, the temperature rose sharply after improving the oxygen supply rate, which caused the calorific value of gas contents to increase continuously, the gas comprised combustible gas compositions of H₂ and CO in high proportions. These results demonstrate that the gasification process and combustion area are expanded. The CO and H₂ compositions were observed to be exhibited a downward trend at about 5 h; the temperatures of thermocouples and gases also tend to decrease at this time, along with the calorific value of gases. At about 6 h, the product gas temperature showed a sudden marked increase. As process proceeded, maximum temperatures also were being recorded by thermocouples CH1, CH2, and CH7 in the cavity space. These data are mainly attributable to the different thermal states of the gasifier achieved during the respective time periods. Changes in the local temperature of the reactor as the gasification process proceeded also affected the concentrations of the production gases.

3 · 1 · 2 L-shaped Linking-hole Model (P7)

Concentration of production gases in relation to the supply rate of gasification agents and the calorific value of L-shaped

linking-hole model experiment are given in Fig. 6.

The oxygen supply rates were changed from 3.8 L/min to 5 L/min during the respective time periods. The combustible gas contents increased rapidly in the early stage. The oxygen supply was changed from 5 L/min to 4 L/min at about 0.5 h; subsequently, the CO, CH₄ composition showed a significant increase. The CO composition is greater than 65%. The calorific value also reached a peak value (17.04 MJ/m³) at 0.9 h. At about 1.4 h after beginning the experiment, the gas stream was ignited successfully. At that time, the oxygen flow rate was improved to the 5 L/min until the end of the experiment. In the next period of about 5 h, the combustion area showed continuous stable gasification. The average calorific value estimated from the product gas was about 11.11 MJ/m³.

Fig. 7 shows the changes in temperature increasing of CH1–CH9, located at different positions (see Fig. 3). The thermocouple CH10 mounted in the production hole detects the gas stream temperature. The temperature recorded at CH2 maintained rapid growth until it reached the highest value (893 °C), which demonstrated that the combustion area was formed near the ignition area (near CH2) in the early stage. Corresponding to the same time period of 0–2 h around Fig. 6, the combustible gas compositions also show a rising trend. Subsequently, the temperatures recorded by thermocouples CH1, CH3, CH5, and CH8 increased prominently. After 2 h and 3 h, thermocouples CH1, CH3 and thermocouples CH5, CH8 gradually rise and respectively reach high levels. Temperatures at CH1 and CH2 show a higher growth rate during 0–2 h. Temperatures at CH5 and CH8 increased rapidly during 4–6 h, as the Fig. shows. It can be inferred that the combustion front moved to the coal block border of the gas outlet side; then the oxygen supply was terminated.

3.1.3 Coaxial-hole Models (P6, P8)

In the laboratory Coaxial-hole model, a coaxial pipeline is set along the vertical-hole (13 mm diameter) to inject oxygen into the combustion reactor. Fig. 3 depicts the dimensions of coaxial tube and the locations of thermocouple arrays with channel numbers CH1–CH7 and CH11. Pure oxygen was supplied to the reaction zone at 3–5 L/min to sustain the gasification process. The gas concentrations and the calorific value of each gaseous product mixture are presented, respectively, in Fig. 8. The combustible gas compositions decreased gradually along with the increase of CO₂ content at about 0.5 h. After the CO₂ contents reached a second peak value (82.4%) and CO decreased, the calorific value also fell to 3.86 MJ/m³ continuously, as the Fig. shows. The oxygen outlet position was moved upward about 50 mm by sliding the inner pipe after about 2.3 h. Then the N₂ contents increased, and the Some of the reactant gas oxygen also bypassed from the injection to production hole, which causes a decrease in cavity propagation. Subsequently, to continue gasification, the oxygen flow rate was increased to 5 L/min. At the time of about 2.8 h and 4.2 h, the oxygen

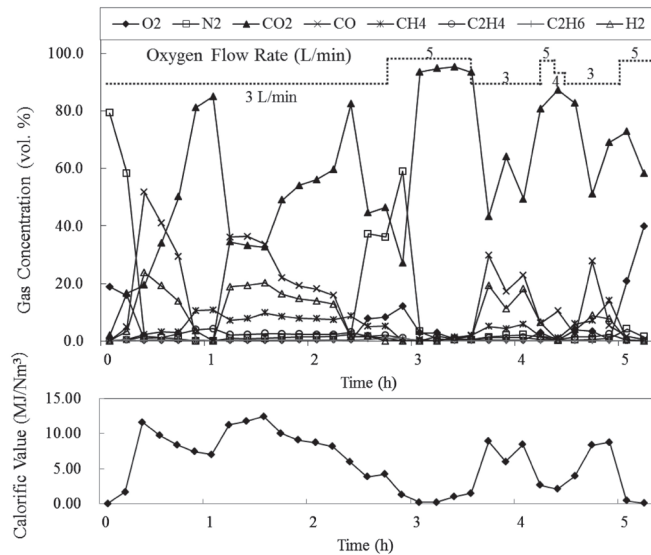


Fig.8 Changes in product gas concentrations during gasification (P6).

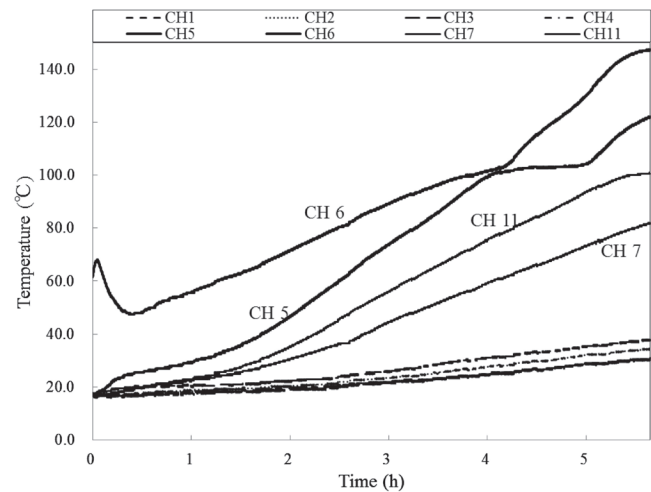


Fig.9 Temperature profile with operational time (P6).

flow rates were also improved to 5 L/min for some time. However, the CO₂ contents increased at high speed. This result demonstrated that the flow rate of 5 L/min was too high for stable gasification under such conditions. Most gas contents aside from CO₂ disappeared. The various product gas quantities fluctuated during the experiment. The average calorific value estimated from these gas contents was about 7.38 MJ/m³ which was only half of the value obtained from Linking-hole model experiments. Stable gasification was inferred not to have occurred in this experiment.

Fig. 9 presents the temperature profiles of the Coaxial-hole model in this work with respect to the operation time. The temperatures detected by each thermocouple were not influenced. During the experiment, only the temperature of the upper part (CH5, CH6) of the coal block increased, as depicted in the Fig.. The temperature of CH5 recorded a local high temperature at about 4 h. The calorific value was also rather high at 8.45 MJ/m³ at this time. The movement of the oxygen outlet did not affect the coal block temperature. As the Fig. shows,

after igniting the coal block, although the temperatures of CH5, CH6, CH7, and CH11 ($CH6 > CH5 > CH11 > CH7$) continued their increase, the remainder of other thermocouples recorded fairly low temperatures during the experiment, meaning that the gasification area was limited to the upper central part of the coal block, with no motion until the end of the experiment.

After the P6 experiment, the coaxial tube was torn down from the model. Then the inner tube of the coaxial pipe was found melted off at the upper part of the coal block. As described previously, the pure oxygen was applied to obtain sufficiently high temperatures necessary for complete combustion and gasification. However, it caused the melting of inner pipe under the high-temperature environment prevailing in the reactor. This melting might be the main reason for a lack of downward movement of the combustion zone. Therefore, the gasification agent was adjusted to an alternative supply of oxygen and air/oxygen mixture in the P8 model. The oxygen ratio of the feed gas mixture is about 35%, which provides a suitable temperature field for coal combustion and which can also prevent the steel inner tube from melting at such high temperatures when pure oxygen was used.

Variations of compositions of all gas components in the P8 UCG model are presented in Fig. 10. The temperature increase of CH2–CH9 measured throughout the combustion process in the coal block is presented in Fig. 11. These results are obtained from the P8 model in which gasification is performed up to about 14 h, and at an average oxygen supply rate of 4 L/min.

The CH9 temperature profile is shown in the Fig., which detected the product gas stream. After beginning, temperatures recorded by thermocouples at CH2 and CH3 maintained a steady increase and arrived at about 100 °C (the temperature of the corresponding coal block surface), which demonstrates that the combustion area was formed near the ignition area (near CH3) in the initial period. After about 3.25 h, the experiment was stopped for about 30 min, which caused a slight drop of temperature and product gas concentration at this time. After about 5 h and 7 h, the temperatures recorded by thermocouples CH2 and CH3 and by thermocouples CH5 and CH6 gradually increased and reached respectively high levels. Furthermore, the combustible gas in H₂ and CO increased by a certain margin and caused a high calorific value (8.24 and 7.32 MJ/m³) in this stage. Thermocouple CH8, which monitors the upper part of the coal block, recorded its highest temperature at about 8.9 h. During the course of the later period, a gradual drop in gasification zone temperatures was observed, reflecting that the reaction area had moved to the coal block border in the upper part. These results demonstrate that the gasification zone had developed. It subsequently moved smoothly from the bottom to the top of the coal block. The horizontal expansion of the combustion cavity was undesirable in the Coaxial-hole model under these experimental conditions.

Production gas produced by Coaxial UCG models during

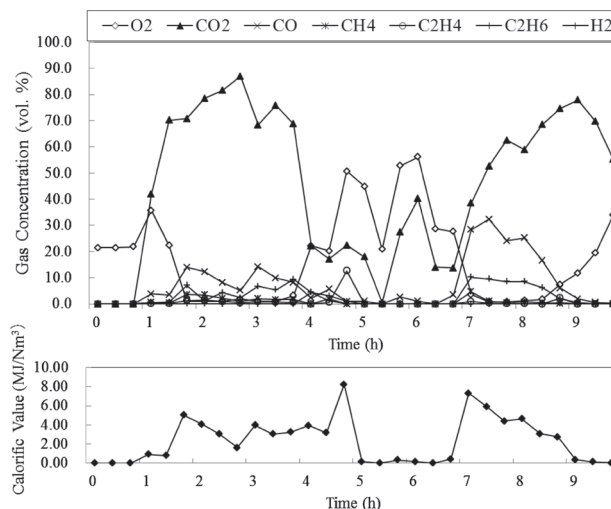


Fig.10 Changes in product gas concentrations during gasification (P8).

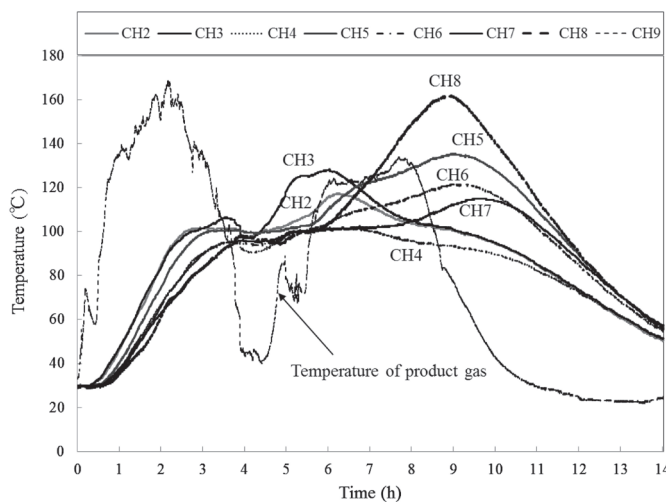


Fig.11 Temperature profile with the operational time (P8).

gasification was insufficient in the quality. The product gas mainly comprised non-combustible components such as CO₂, N₂, and the bypassed O₂, although combustible components showed a larger fluctuation during the experiment. This lack of combustible components yielded a relatively low average calorific value (7.38 and 4.70 MJ/m³) of the product gas.

3 · 2 Small-scale Field Tests

3 · 2 · 1 Test Field and Coal Over the past century, although many field trials have been described in the literatures, few data are available for gasification evaluation because of the trials' complex control, time-consuming processes, and high costs. The need persists to obtain experimental data related to evaluation of gasification effects and product gas calorific values with respect to a given set of design and operating conditions. Therefore, based on the UCG laboratory experiments described above, small-scale field tests of the Linking-hole and Coaxial-hole models were performed, respectively, at an open-cut Coal Mine (Sunago) in Hokkaido. Two field trials were conducted to assess the feasibility of the UCG process for a selected coal seam under the specified conditions. The results of proximate

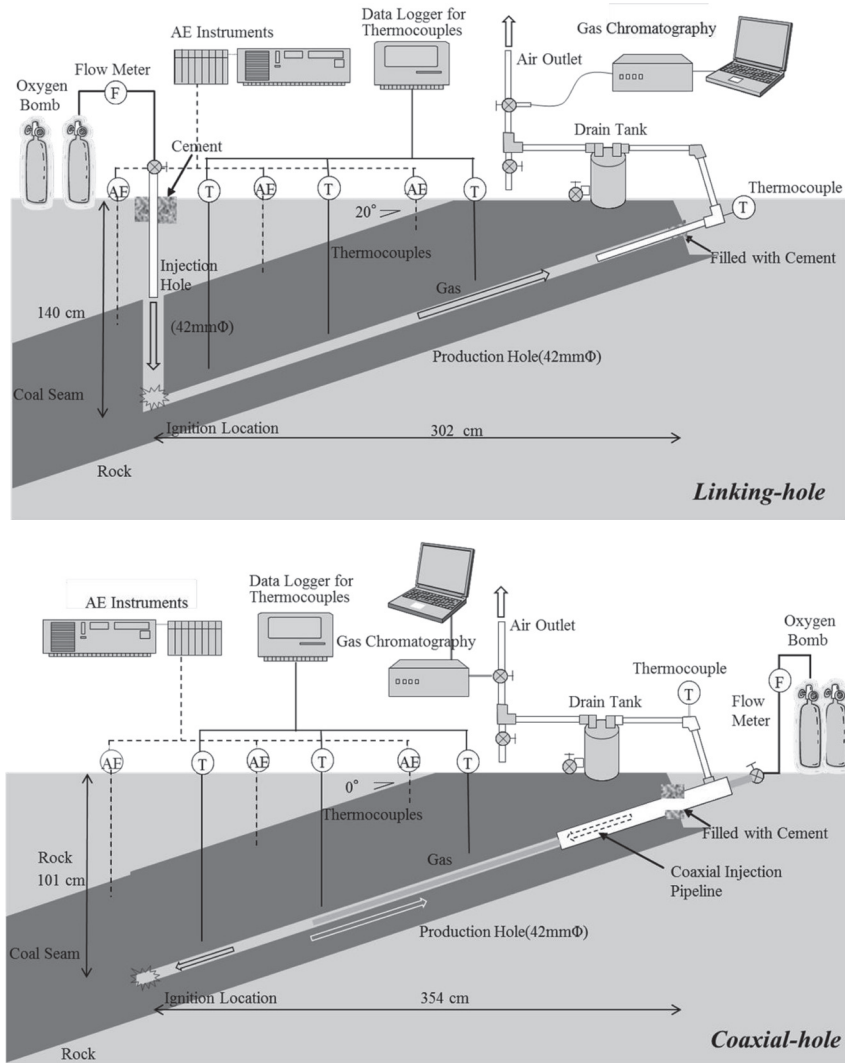


Fig.12 Scheme of the experimental setup used in the field tests.

and ultimate analysis of the coal under study are presented in Table 1. The coal is a highly volatile (37.97%) bituminous coal with high fixed carbon content (41.41%) .

3 · 2 · 2 Experimental Setup

Schematic diagrams showing the structure of the underground gasifier used in field trials are presented in Fig. 12. The thermocouples locations used for Linking-hole and Coaxial-hole tests are shown respectively in Fig. 13. In these two systems, underground coal gasification was conducted using oxygen as the gasification agent. The Linking-hole model gasifier has an injection hole and a production hole (gasification channel) . In the Coaxial model test, the coaxial pipeline was set into the coal seam. The oxygen was blown into the underground through the inner pipe and the gas outlet by the outer pipe. The gasifiers used similar measuring apparatus from those used in laboratory experiments, but used different operational parameters. An exception is that the product gas was sampled and analyzed using gas chromatography every 30 min (occasionally 1 h where necessary) . The net diameters of boreholes were 0.42 m, with vertical depths of 1.4 m (Linking-hole) and 1.01 m (Coaxial-hole) .

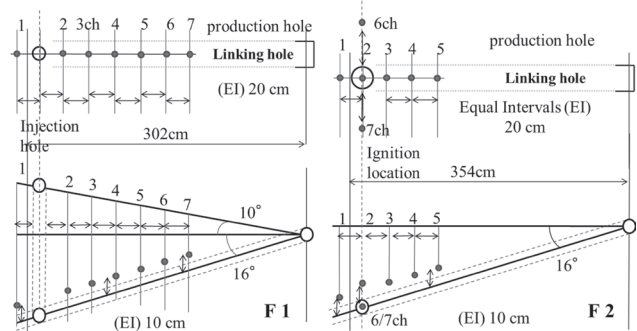


Fig.13 Locations of thermocouples in the field.

3 · 2 · 3 Experimental Results For the Linking-hole field test, only pure oxygen was supplied (flow rate of 20 L/min) into the reaction zone. The combustion process proceeded for 39 h, yielding continuous and stable gasification. The temperature distribution inside the underground reactor and product gas concentration with respect to the operation time are presented respectively in Fig. 14 and Fig. 15. The thermocouple at CH8 shows gas product stream temperature. The O₂ composition rose

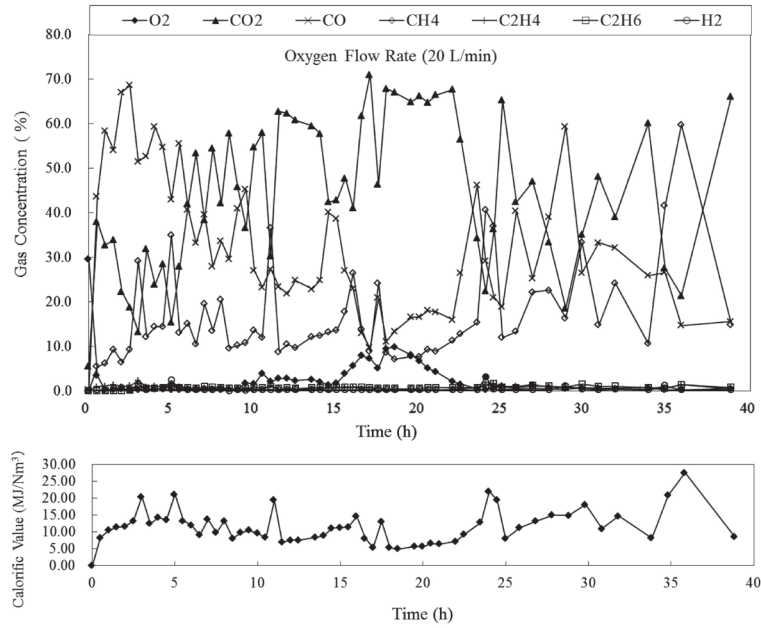


Fig.14 Changes in product gas concentrations in the linking-hole field test.

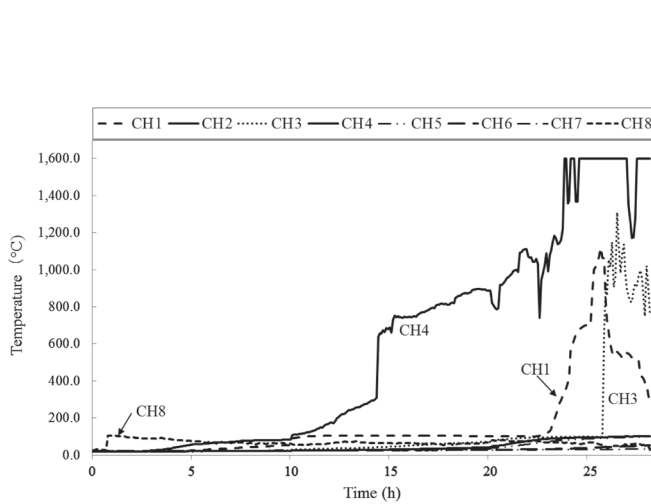


Fig.15 Temperature profile with the operational time in the linking-hole field test.

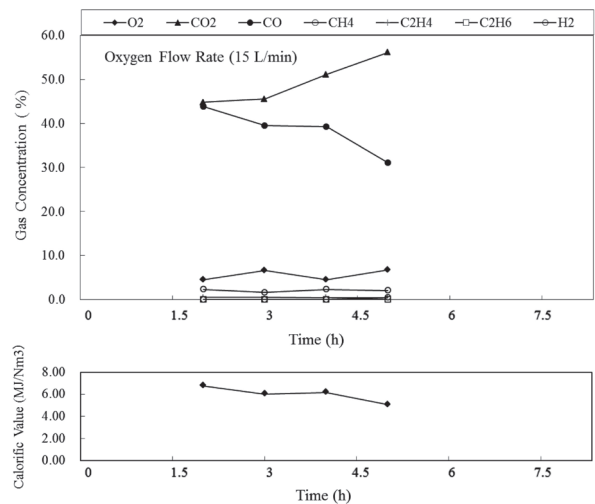


Fig.16 Changes in product gas concentrations in the coaxial field test.

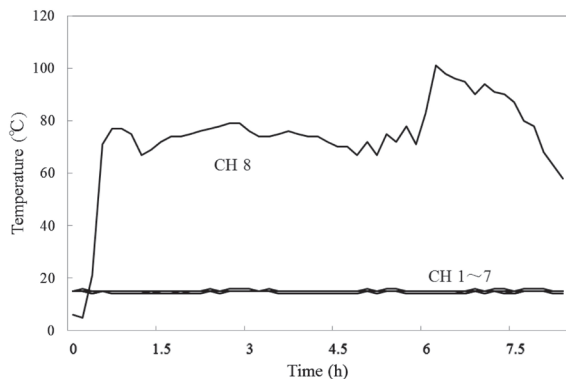


Fig.17 Temperature profile with the operational time in the coaxial field test.

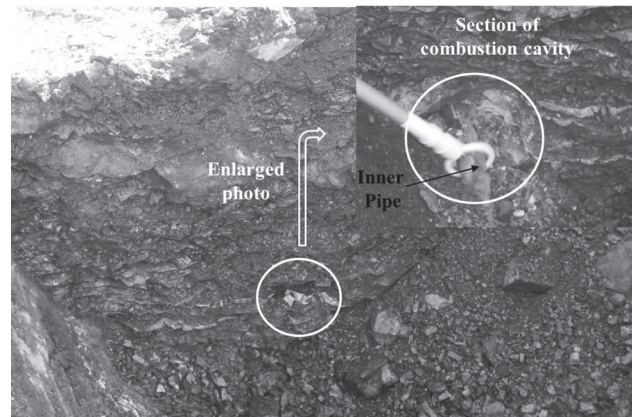


Fig.18 Section photographs of a gasification cavity of a coaxial UCG test.

after about 10 h. The calorific value was at a lower level. For this period, the gasification process maybe dropped for a short while. The combustion area also decreased. The average calorific value of the product gas was 14.39 MJ/m³.

The flow rate of pure oxygen was adjusted to the 15 L/min and was kept constant for the entire duration of the Coaxial UCG field test. Fig. 16 and 17 respectively present the temperature profiles and the changes of gas compositions in the Coaxial test. After igniting the coal seam, a low average calorific value (6.66 MJ/m³) was obtained during the approximately 9 h gasification processing. Product gas compositions were not detected successfully in the first period (about 120 min) because of a transient fault of the gas chromatography instrument, which caused failure in analyzing the gas samples. However, the existence of flammable production gas in this phase was confirmed. After about 300 min, the monitoring instrument malfunctioned once again. At this time, the gas chromatograph was unable to function normally work because of the under pressure of helium carrier gas cylinder, which was affected by the sudden drop of the air temperature.

Results show that the temperatures recorded at CH1–CH7 were low level (14–16 °C) throughout the gasification process. After igniting the coal seam, only the temperature at CH8 (product gas temperature) increased sharply and reached a high level. Temperatures around the coaxial hole were lower because combustion occurred only near the coaxial hole. The thermocouples were distant from the combustion area.

We observed the underground combustion zone directly by removing the overlying strata using an excavator when the experiment was completed. The combustion cavity was limited around the gasification channel: effective combustion had not progressed. This result can be confirmed by section photos of the combustion cavity, as shown in Fig. 18. This small combustion cavity indicated that only a small free coal face was exposed to the reactant gases for additional gasification. This relation is similar to those found in the results of laboratory experiments.

4. Discussions

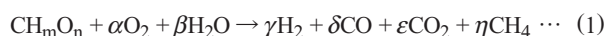
Above described experiments for simulating underground coal gasification were conducted to evaluate the gasification efficiency. The four laboratory experiments were conducted using coal blocks with different linking-hole type systems (V-shaped, L-shaped, Coaxial) , yielding results of temperature profiles, product gas variations, average calorific values, and gasifier weight loss. Pure oxygen was applied as a gasification agent, except for P8 model experiments. Two small-scale field tests of the Linking-hole and Coaxial-hole models were conducted in underground coal seams. Similar process results were measured under oxygen injection conditions. From data of gas composition measurements and temperature profiles, it can be concluded that high calorific values and appropriately stable works of reactor were achieved in the Linking-hole UCG tests. To elucidate the gasification mechanism and estimate the different gasification effects of the experiments described above, we evaluated the gas energy recovery and gasification cavity as explained in the following sections.

4 · 1 Evaluation of Energy Recovery

Each UCG system exhibits distinct gasification progress and cavity growth phenomena because of the coal properties and operating parameters in the process of generating syngas. The cavity formation and gasification efficiency at any operating time depends on the quantity and rate of coal consumption and assessment of underground conditions, although obtaining such information is not practical if done in-situ. Furthermore, underground coal gasification entails energy loss in various forms of surface leakage, heat loss to the surroundings, conversion of inherent moisture into water vapor, and so on.

Circumstances related to underground target coal seams in the UCG work can be estimated using a method of the reaction process of coal gasification from the composition of gas produced and reacted amounts of O₂ and H₂O that have been investigated²⁰⁻²²). Moreover, as a necessary parameter for evaluating the underground cavity, and the efficiency and safety of UCG, coal consumption during the gasification process can be estimated using this stoichiometric approach. These experiments have facilitated gasification reaction calculations from gas compositions and results of coal elemental analysis. We specifically examined comparison of the chemical processes of various gasification designs. This method is universally applicable to the gasification phenomena because it incorporates no assumption or approximation for the calculation formula. Therefore, this analytical method is suitable for the estimation of underground gasification reactions in the UCG trials that have sufficient fundamental data including the product gas composition and elemental analysis values. Few reports in the literature have described analyses, few data have been obtained from analyses of the reaction formula from the gasification reaction processes created based on the generated product gas composition.

We investigated this method to estimate the gasification process represented by deriving the UCG chemical reaction with O₂ and H₂O as gasification agents. This stoichiometric method is proposed to analyze this reaction process of coal gasification. Equation (1) shows that chemical reactions that occur during the gasification process can be expressed as a material balance equation as shown in. Herein, the chemical process might be discussed sufficiently based on the CH_mO_n irrespective of the detailed structure of coal molecule. The dry and clean syngas produced from the UCG process used in this formula contains H₂, CO, CO₂, and CH₄ (N₂ free) , of which the concentrations are respectively represented by *p*, *q*, *r*, and *s*. In the present works, the trace gases of propene and propane compositions accounted for a proportion in synthesis gas. In the following calculation, the values of *p*, *q*, *r*, and *s* are taken to be average values (see Table 3) , obtained from gas analysis results.



Therein, α and β are balance coefficients of O₂ and H₂O, and *m* and *n* are given by ultimate analysis of coal samples. Also γ , δ , ε and η are the respective gas outputs of H₂, CO, CO₂, and CH₄. Let the total moles of product gases in Eq. (1) be equal to Σ .

$$\Sigma = \gamma + \delta + \varepsilon + \eta \cdots \cdots \cdots (2)$$

Table 3 Average gas compositions of product gases in these studies.

Average gas composition	O ₂	N ₂	CO ₂	CO	CH ₄	C ₂ H ₄	C ₂ H ₆	H ₂
	%	%	%	%	%	%	%	%
V-shaped (P2)	0.3	2.8	45.7	28.9	5.7	0.0	1.9	17.8
L-shaped (P7)	0.6	2.0	45.9	32.3	11.2	3.5	0.5	6.7
Coaxial (P6)	4.1	7.2	68.6	15.0	5.4	1.8	0.3	8.9
Coaxial (P8)	17.6	17.4	80.7	11.2	1.2	1.6	0.6	4.4
Field(link)	2.1	2.0	47.4	33.7	17.3	0.6	0.7	0.4
Field(coaxial)	5.6	3.9	54.6	42.4	2.3	0.5	0.0	0.1

Table 4 Calorific values of combustible gas components (dry).

Gas Component	H ₂	CH ₄	C ₂ H ₄	C ₂ H ₆	CO
Calorific Value MJ/m ³	12.8	39.9	63	69.7	12.6

The mole number of each gas compositions γ - η is described as follows,

$$\gamma = p\Sigma; \delta = q\Sigma; \varepsilon = r\Sigma; \eta = s\Sigma \dots \dots \dots (3)$$

$$p + q + r + s = 1 \dots \dots \dots (4)$$

By substitution into the carbon equilibrium equation ($1 = \delta + \varepsilon + \eta$) of Eq. (1), the total moles are obtainable as

$$\Sigma = 1 / (q + r + s) \dots \dots \dots (5)$$

From the average concentrations of each gas, we have the following,

$$\gamma = p / (q + r + s); \delta = q / (q + r + s); \varepsilon = r / (q + r + s); \eta = s / (q + r + s) \dots \dots \dots (6)$$

The decomposition amount of H₂O (β) can be obtainable by substituting Eq. (6) into the hydrogen equilibrium equation ($m + 2\beta = 2\gamma + 4\eta$) of Eq. (1), as shown below.

$$\beta = (p + 2s) / (q + r + s) - 1/2m \dots \dots \dots (7)$$

Substitution of Eq. (6) and Eq. (7) into the oxygen equilibrium equation ($\eta + 2\alpha + \beta = \delta + 2\varepsilon$) of Eq. (1), gives the balance coefficient of O₂, α , as

$$a = (q + 2r - p - 2s) / (2(q + r + s)) + (0.5m - n) / 2 \dots \dots \dots (8)$$

The quantity of coal consumption (A) kg/h is determined from the amount of O₂ supply (S) m³/h and balance coefficient α (Eq. (8)) as shown below.

$$A = (S \times M \times 1.2 \times 1000) / (22.4 \times (C\%) \times a) \dots \dots \dots (9)$$

Therein, M is the mole fraction of O₂ ($M=1$ when pure oxygen is used as the gasification agent in the UCG work). Also, $C\%$ is

the carbon content taken by ultimate analysis.

The amount of dry gas flow (m³/h) is calculated as shown below.

$$G = \Sigma \times C_m \times 0.0224 = \Sigma \times (A \times C\% / 1200) \times 0.0224 \quad (10)$$

In this equation, C_m is the mole amount of coal consumed through the gasification process; A is the quantity of coal consumption (Eq. (9)) in grams.

Table 1 presents proximate analysis and ultimate analysis of the coal used for this study. The average gas compositions of the product gas in the experiments and small-scale field tests are shown in Table 3. The percentages of hydrogen output in the laboratory experiments that used Kushiro coal were 4.4–17.8%, but Sunago coal used in field tests produced hydrogen composition of only about 0.1–0.4%, probably because the Kushiro coal provided more moisture for the coal reduction reactions. Some carbon dioxide and water were reduced to carbon monoxide and hydrogen. In addition, the temperature of reactor had a rather high temperature field even more than 1600 °C. It went against the occurrence of reduction reactions, because the reduction of CO₂ and decomposition of moisture could occur with a temperature of about 600–1000 °C^{23, 24}. The component contents of C, H, N, and O in different coals affect m , n , $C\%$, thereby directly affecting the energy recovery results.

The percentage of gas composition was calculated through the correction computation of water removal from the product gas that had been analyzed directly using gas chromatography. The calorific value of each content gas is presented in Table 4. Furthermore, the calorific value was calculated using the Eq. (13), based on various combustible gas components under the dry and standard state.

Table 5 Estimated results of coal consumption and product gases.

Pilots Linking-hole Type	Laboratory Experiments				Field Trials	
	V-shaped (P2)	L-shaped (P7)	Coaxial (P6)	Coaxial (P8)	Linking-hole	Coaxial-hole
p(H ₂)	0.178	0.067	0.089	0.044	0.004	0.001
q(CO)	0.289	0.323	0.150	0.112	0.337	0.424
r(CO ₂)	0.457	0.459	0.686	0.807	0.474	0.546
s(CH ₄)	0.057	0.112	0.054	0.012	0.173	0.023
m(CH _m O _n)	1.002	1.002	1.002	1.002	0.891	0.891
n(CH _m O _n)	0.143	0.143	0.143	0.143	0.092	0.092
C%	65.53	65.53	65.53	65.53	67.59	67.59
Oxygen flow rate avg.[m ³ /h]	0.40	0.29	0.21	0.28	1.20	0.90
Time [h]	8.00	8.43	5.17	8.67	38.83	9.00
Calorific value [MJ/m ³]	10.26	11.11	7.38	4.70	14.39	6.66
Mole-fraction (O ₂)	1	1	1	1	1	1
α	0.727	0.710	0.895	1.056	0.651	0.916
Rate of coal consumption [kg/h]	0.475	0.344	0.188	0.228	1.763	0.779
Total amount of coal consumption [kg]	3.800	2.902	0.971	1.977	68.467	7.015
Quantity of gas product						
/ Time [m ³ /h]	0.753	0.471	0.266	0.304	2.276	0.990
Total volume [m ³]	6.023	3.971	1.372	2.632	88.380	8.911
/Coal [m ³ /kg]	1.585	1.368	1.412	1.331	1.291	1.270
Calorific value of gas product						
/Time [MJ/h]	7.728	5.756	1.960	1.428	32.753	6.590
Total amount [MJ]	61.821	44.128	10.128	12.376	1271.914	59.309

$$H_V = V_{H_2} \times 12.8 + V_{CH_4} \times 39.9 + V_{C_2H_4} \times 63.0 + V_{C_2H_6} \times 69.7 + V_{CO} \times 12.6 \dots\dots\dots (11)$$

In this equation, the H_V denotes the calorific value of the product gas mixture. Wherein, V_{H_2} , V_{CH_4} , $V_{C_2H_4}$, $V_{C_2H_6}$, and V_{CO} respectively express the percentage compositions (mole percent) in the gas mixture with respect to the operation time.

This method specially estimated of energy recovery outcomes such as coal consumption, product gas quantity, and produced heating value. It also assessed the effects of linking methods and related operational parameters.

Detailed results of gas energy recovery and relevant parameters in these works are presented in Table 5. The total amounts of coal consumed in the Linking-hole and Coaxial-hole models of laboratory experiments were, respectively, 3.800 kg (V-shaped), 2.902 kg (L-shaped), and 0.971 kg (Coaxial, P6), 1.977 kg (Coaxial, P8). As presented in the table, the rate of coal consumption in the Coaxial-hole field test was about 0.779 kg/h, which equals about half of the value obtained in the Linking-hole test (1.763 kg/h). During all tests, the coal

consumed in the field is predicted as about 68 kg for 39 h and 7 kg for 9 h. The amounts of gas production and calorific values obtained from these experiments are also calculated with the quality of coal consumption. The Coaxial-hole system gas exhaust rate was 0.990 m³/h, much lower than 2.276 m³/h of the Linking-hole test.

The calorific values of product gas obtained in the conducted models are shown in Fig. 19. The higher calorific value were produced more and faster in the Linking-hole UCG models, whereas the experiments conducted with Coaxial UCG model yielded low calorific values. In addition, the average values of the calorific value and offtake rate in the laboratory-scale tests are also less than the results obtained from the small-scale field test. Compared with the natural underground coal seam, the coal blocks used in the laboratory experiments have higher density and hardness, which might have reduced the cavity growth rates and produced lower calorific values. In the field test, the higher crack porosity and natural fissures of the coal body are more beneficial to the gas flow and coal combustion around the gasifier. The oxygen flow rate in the

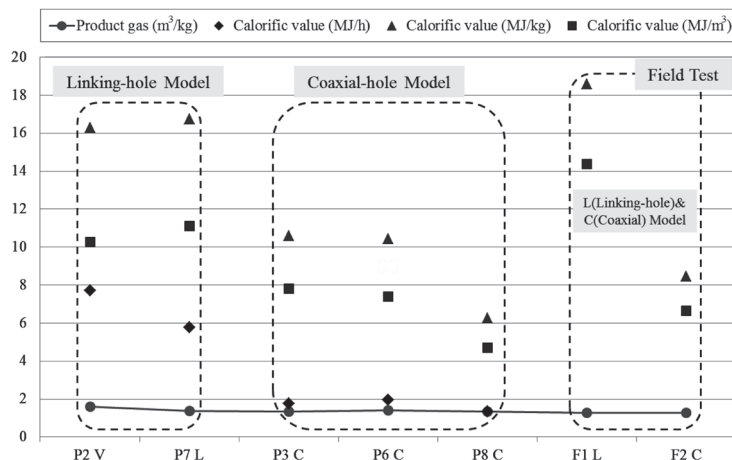


Fig.19 Calorific values with these UCG models.

Table 6 Calorific values of product gases obtained during UCG trials.

Pilots	Laboratory Experiments		Field Tests		Abroad pilots		
	linking-hole	coaxial-hole	linking-hole	coaxial-hole	Rocky Mountain1 (USA)	Angren (Uzbekistan)	Lisichansk (Ukraine)
Calorific value [MJ/m ³]	10.26-11.11	4.70-7.38	14.39	6.66	8.80-9.50	2.30-3.80	3.77-10.46

case of laboratory experiments is also lower by about 25–60% than the value supplied in field tests. Moreover, in the present experiments, the highest temperature of the combustion zone in the laboratory UCG models was only about 900–1000 °C, but the temperature in-situ exceeded 1600 °C under the experimental conditions. Another interesting finding is that the amounts of the product gas gasified from the consumed coal show a similar result, which also reconfirmed the availability of the estimated results of gas energy recovery.

The calorific values of the gas produced in the UCG experiments are presented in Table 6. For comparison, the results of typical UCG trials^{1, 25)} conducted throughout the world are also shown. It can be seen that the average calorific values of product gas obtained in the Linking-hole UCG experiments are between 10.26–14.39 MJ/m³, which is of the same order as results of field UCG conducted in the Rocky Mountains (USA) and in Lisichansk (USSR). Even though the Coaxial UCG in our study produced relatively low calorific values, compared to the UCG works in Uzbekistan that also show fairly good results.

To evaluate the gasification effect, the cavity volumes of the L-shaped model and two Coaxial models were also investigated. After the experiment, the connecting pipelines were torn down and the plaster was poured into the reactor to facilitate observation of the cavity shape and cracks. Fig. 20 portrays the photographs of vertical sections of the Coaxial models. The sections of the L-shaped model are cut parallel to the directions given in the Fig.. The white area shows the cavity and cracks cemented by plaster. The areas of the irregular

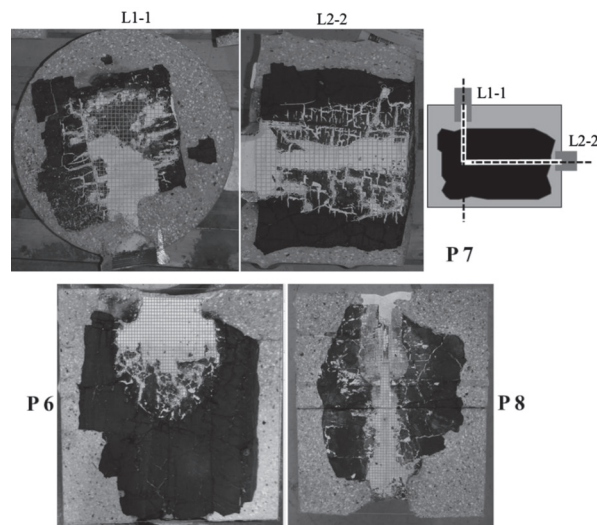


Fig.20 Cutting sections of the L-shaped model (P7) and Coaxial models (P6/P8).

plane Fig.s of cavity sections are obtainable. Furthermore, the approximate value of volume (v_1) was obtainable through calculation the three-dimensional cavity obtained by revolving the irregular plane of the cavity section. Another method is calculation of the cavity volume (v_2) using the actual weight loss of the model. This result may be affected by the internal micro-cracks inside the coal. The cavity volume results are summarized in Table 7.

Moreover, the relations between the calculated prediction of coal consumptions and the experimentally obtained results were also compared. Table 8 gives the actual value of the weight shortage in each laboratory experiment. The error

Table 7 Cavity volumes in the UCG models.

Linking-hole type	L-shaped P7	Coaxial P6	Coaxial P8
Cavity Volume v1 (cm ³)	3672.4	1683.1	1846.4
Cavity Volume v2 (cm ³)	3128.5	1128.6	1673.2

Table 8 Actual values of model weight loss with correlation predictions.

Linking-hole type	V-shaped P2	L-shaped P7	Coaxial P6	Coaxial P8
Correlation Predictions (kg)	3.800	2.902	0.971	1.977
Actual Weight Loss (kg)	4.220	3.285	1.065	2.125
% Error	9.953	11.659	8.826	6.965

Table 9 Rates of energy recovery in these UCG model experiments.

Linking-hole Type	P2	P7	P6	P8	F1	F2
Gas Production Rate [m ³ /kg]	1.585	1.368	1.412	1.331	1.291	1.270
Unit Calorific Value [MJ/m ³]	10.26	11.11	7.38	4.70	14.39	6.66
Calorific capacity [MJ/kg]	26.15	26.15	26.15	26.15	25.43	25.43
Gasification Rate [%]	62.19	58.12	39.85	23.92	73.05	33.26

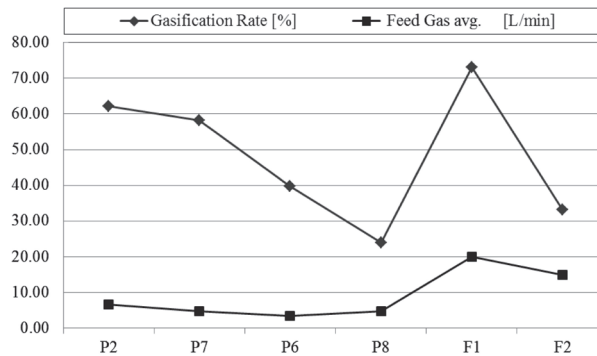


Fig.21 Comparison of rates of gasification and feed gases in these experiments.

percentages are presented in the Table, which shows that the maximum percentage error between the experimental values and the estimations is only about 10% for these different models. The error value might result from moisture evaporation within the coal (inherent moisture) and not dry concrete, the tar filtered by the purification system, and the volatile matters.

The applied coal blocks and target coal seams have differing calorific capacities. To evaluate the energy exchange efficiency in these experiments better based on the stoichiometric results, a definition of the energy recovery rate (R_g) was proposed as a function of the calorific capacity (Q_c) and two independent variables: the dry gas production rate (V_d) and the unit calorific value (Q_u). The rate of gasification might be written as shown below.

$$R_g = (V_d \times Q_u) / (Q_c) \times 100\% \dots\dots\dots (12)$$

A comparison of the results is presented in **Table 9**. Correlations between feeding gas injected in these UCG processes and the estimated gasification rate are presented in **Fig. 21**.

4 • 2 Linking UCG and Coaxial UCG

The experimentally obtained results of Linking and Coaxial UCG models are discussed in the sections above based on observations of temperature profiles (cavity growth) and product gas concentrations. Evaluation of energy recovery reconfirmed this result. The experiments proved the efficient combustion, cavity propagation, and high quantity of synthesis gas obtained in the Linking UCG models. The Coaxial UCG limited the combustion zone to the region circumjacent to the coaxial hole. Consequently, a low heating value was observed.

As described previously, Coaxial UCG is anticipated for use as a local energy source in small communities because the costs to construct the drill hole and ground plant facility are

Table 10 Fissure ratios around gasification channel in laboratory UCG models.

Linking-hole type	V-shaped P2	L-shaped P7	Coaxial P6	Coaxial P8
Fissure Ratio [%]	30.37	27.79	16.25	10.28

lower than those for conventional UCG with a linking hole.

However, because of the operational characteristics of the Coaxial UCG system, the open heading of the drill hole might be plugged. The ash at the bottom of the cavity hinders the further gasification reaction by acting as a barrier against heat and gas transfer. Moreover, the ceramic concentric air/oxygen pipe (inner pipe) used in the Coaxial UCG is liable to fracture (ceramic pipe in P6) or burn away (steel pipe in P8) because of fragility or high temperatures. Therefore, contrary to our expectation, the reaction in the gasifier invariably ceased prematurely. Inspections revealed that large parts of the inner pipe had been broken up or burned away.

In addition, the constant high temperatures and slow cavity propagation in the reactor of Coaxial UCG experiments formed a harder semi-char zone and char zone, thereby raising the physical and mechanical intensity of the coal body around the gasifier. This phenomenon also hinders further combustion during the gasification process. For further validation, we also investigated the fissure ratios of laboratory UCG models that were obtained from the cross section images. Table 10 presents the fissure ratios, i.e. proportion of blasting-induced cracking zone per unit area, around the linking holes.

Future studies shall examine the design of a mechanical agitating and grinding device of gasification cavity for expansion of the oxidation surface around the bottom of the coaxial-hole, thereby improving the effective combustion and gasification efficiency in Coaxial UCG.

5. Conclusions

These present experimental and small-scale field studies of UCG were conducted to evaluate the gasification effect and gas energy recovery by distinct design models. Through comparison of the process results, the investigation revealed that the linking methods and operational parameters strongly influence the cavity volume and gasification effects. The following conclusions can be drawn from this study:

- (1) By performing coal gasification in the laboratory and in-situ used Linking-hole models, we obtained a high average calorific value of product gas, in which CO is greater than about 30% and CH₄ is even rather high at 17%, with the average calorific value of about 14 MJ/m³. Although the scale of our studies were conducted on a smaller than an industrial scale, they have yielded useful data for reference in support of field UCG.
- (2) Laboratory experimental results indicate that gasification integrates with oxygen because the gasification agent provides a sufficient temperature field for effective combustion and cavity growth. Furthermore, to produce a greater degree of gasification, the oxygen supply rate should

be controlled in a reasonable range at different stages.

- (3) Although the Coaxial UCG system has certain marked advantages over Linking UCG, monitoring results obtained in these experiments demonstrate that the combustion zone is fairly localized in the Coaxial UCG models. The zone is circumjacent to the gasification channel under experimental parameters.
- (4) As an important index of UCG effects, the cavity volume was investigated combined with fissure ratios around the gasification channel inside these models. Results for the cavity volume formed in the laboratory Coaxial models were only half those of the data obtained for the Linking-hole model.
- (5) Evaluation of gas energy recovery elucidates the gasification reaction process based on the stoichiometry using gas compositions obtained from this study. The stoichiometric method is simple, efficient, and estimates the gasification cavity formed inside UCG model well. As an evaluating indicator, the rate of energy recovery was defined and calculated. These estimated results show proven effectiveness and provide a fair evaluation of coal consumption while showing some conditions for use of the UCG process in target coal seams.

Future studies must find or develop alternative heat-resistant materials for use in the inner tube, mean to control the temperature field by adjusting the air/oxygen input ratios, and techniques for expanding the combustion zone for all methods aside from the efficient Coaxial UCG.

Acknowledgments This work was supported by the Japanese Society on UCG, Mikasa City, Center of Environmental Science and Disaster Mitigation for Advanced Research of Muroran Institute of Technology and a Grant-in-Aid for Scientific Research (b) , 21360441 from the Ministry of Education, Culture, Sports, Science and Technology (MEXT) , Japan. The authors gratefully acknowledge their support.

References

- 1) E. Burton, J. Friedmann, and R. Upadhye: Best practices in underground coal gasification. Draft. US DOE contract noW-7405-Eng-48. CA, USA, Livermore: Lawrence Livermore National Laboratory, 2006.
- 2) E.B. Kreinin: Two-stage underground coal gasification. *Coal Chem. Ind.* **6** (3) (1993), 61-63.
- 3) F.H. Franke: Survey on experiment laboratory work on UCG, In: Proceedings of the 12th Annual Underground Coal Gasification Symposium, Washington, DC, USA, 1986. pp. 131-133.
- 4) L. Yang, S. Liu, L. Yu and J. Liang: Experimental study of shaftless underground gasification in thin high-angle coal seams. *Energy Fuels*, **21** (2007), 2390-2397.
- 5) C.B. Thorsness and J.A. Britten: Analysis of material and energy balances for the rocky mountain-1 UCG field test. Report No. 44-49. U.S. DOE, W-7405-Eng-48. Livermore, CA: Lawrence Livermore National Laboratory; 1984.
- 6) B. Debelle and M. Malmendier: Modeling of flow at Thulin underground coal gasification experiments. *Fuel*, **71** (2) (1992), 95-104.
- 7) F.E. Thomas: Research and development on underground gasification of Texas lignite. In: William BK, Robert DG, editors. *Underground coal gasification: The state-of-the-art*, vol. 79. New York: American Institute of Chemical Engineers; 1983. pp. 66-77.

8) V. Chandelle: Pushing through project of the gasification channel in Tulin coal field. Min. Technol, **13** (2) (1992), 5-7 [Collections of Translated Works].

9) N. Hossein, K. Mohammad, C. Zhangxin, and A. Jalal: Simulation study of underground coal gasification in alberta reservoirs: geological structure and process modeling. Energy Fuels, **24** (2010), 3540-3550.

10) P. Alexander, T. Coots, and B. David: comparative study of the measuring methods adopted in the gasification of horizontal and steep coal layers. Min. Technol., **5** (2) (1985), 107-115 [Collections of Translated Works].

11) G. Perkins and V. Sahajwalla: Mathematical model for the chemical reaction of a semi-infinite block of coal in underground coal gasification. Energy and Fuels, **19** (2005), 1679.

12) G. Perkins and V. Sahajwalla: Numerical study of the effects of operating conditions and coal properties on cavity growth in underground coal gasification. Energy Fuels, **20** (2006), 596-608.

13) L. Yang: Study on the model experiment and numerical simulation for underground coal gasification. Fuel, **83** (2004), 573.

14) C.B. Thorsness and R.B. Rosza: In situ coal gasification model calculation and laboratory experiments. Soc Pet Eng J., **18** (1978) 105-116.

15) P.N. Thompson: Gasifying coal underground. Endeavour **2** (1978), 93.

16) M.S. Blinderman, D.N. Saulov, and A.Y. Klimenko: Forward and reverse combustion linking in underground coal gasification. Energy, **33** (2008), 446.

17) D. Gregg: Relative merits of alternate linking techniques for underground coal gasification and their system design implications. Report No. UCRL- 82112.U.S.DOE. Livermore, CA: Lawrence Livermore National Laboratory; 1980.

18) D. Gregg and T.F. Edgar: Underground coal gasification. AIChE J., **24** (1978), 753.

19) S. Faqiang, T. Nakanowataru, K. Itakura K. Ohga, G. Deguchi: Evaluation of Structural Changes in Coal Specimen Heating Process and UCG Model Experiment for Developing Efficient UCG System. Energies, **6** (5), 2386-2406, 2013.

20) M. Kaiho, H. Yasuda and O. Yamada: A method of estimating the reaction process of coal gasification from the composition of gas produced. Proc. of 45th Conf. of the Coal Science. (45), pp.60-61, 2008.

21) M. Kaiho, H. Yasuda and O. Yamada: Evaluation of coal gasification reaction from composition of gas produced. Proc. of 18th Conf. of the Japan Institute of Energy. (18), pp. 28-29, 2009.

22) M. Kaiho and O. Yamada: Stoichiometry and Materials Science - When Numbers Matter, (2012), 415-436.

23) A.W. Bhutto, A.A. Bazmi, G. Zagedi: Underground coal gasification: From fundamentals to applications. Progress in Energy and Combustion Science, **39** (2013) 189-214.

24) L. Yang, D. Song: Study on the method of seepage combustion in under-ground coal gasification. Xuzhou, China: China University of Mining and Technology Press; 2001.

25) A. Beath, et al. Underground coal gasification: evaluating environment barriers. CSIRO Exploration and Mining report P2004/5, Kenmore, Queensland, Australia, CSIRO Publishing, 2001, pp. 1307-1312.

室内および小規模フィールド実験による石炭地下ガス化 (UCG) のエネルギー回収率評価*

蘇 發 強¹ 板 倉 賢 一² 出 口 剛 太³
大 賀 光 太 郎⁴ 海 保 守⁵

UCG においては、炭層内のき裂進展に伴う燃焼空洞の拡大と石炭の消費が重要であり、これがガス化効率や安全性（地盤沈下、ガス漏洩等）に大きく影響する。本研究では、ガス化効率、回収エネルギーとガス化空洞の評価方法として、化学量論および化学平衡に基づく評価手法を検討した。生成ガス組成と求めたガス化反応式から、石炭の消費量、ガス生産量等を推定する方法である。また、エネルギー回収率を定義し、UCG 室内モデル実験及び露天炭鉱の炭層で行った小規模現場実験の結果を評価し、リンクングの方式や注入ガス等のパラメータがガス化効率やガス化空洞の成長に与える影響を検討した。

リンクングの方式として、L 字、V 字、同軸型の UCG 実験を行い、ガス化効率の違いと、その原因を明らかにした。すなわち、リンクング型と同軸型モデルを比較すると、リンクング型 UCG モデルの方が発熱量が高く、平均発熱量では、前者が 10.26/11.11 MJ/m³（室内）、14.39 MJ/m³（現場）であった。一方、同軸型モデル試験では、7.38/4.70 MJ/m³（室内）と 6.66 MJ/m³（現場）と低い値であった。実験後の空洞体積の直接評価結果でも、リンクング型の方がガス化領域が拡大していることを確認した。リンクング方式の

方が、炭層内にき裂を連続的に進展させやすいためと考えられる。

また、エネルギー回収率の評価では、実験前後の供試体質量差から求めたエネルギー回収率と比較検討を行った。その結果、両者の誤差は約 10%で、検討した手法によりエネルギー回収率や燃焼ガス化領域の石炭消費量を推定できることがわかった。

以上の結果より、検討した化学量論法による回収エネルギー評価手法は簡便で、実用的であることが明らかになった。

*2014 年 9 月 29 日受付 2015 年 4 月 10 日受理
[著者連絡先] FAX: 0143-46-5499

Email: itakura@mmm.muroran-it.ac.jp

1. 正会員 室蘭工業大学 環境科学・防災研究センター 博士研究員 博士 (工学)
2. 正会員 室蘭工業大学 大学院工学研究科 教授 工学博士
3. 正会員 NPO 法人 地下資源イノベーションネットワーク 理事長 工学博士
4. 正会員 北海道大学 工学研究院 環境循環システム部門 助教 工学博士
5. (独) 産業技術総合研究所 エネルギー技術研究部門 工学博士
キーワード: 石炭の地下ガス化, UCG モデル, ガス化効果, 石炭消費量, 回収エネルギー